Environ Earth Sci (2016) 75:506
DOI 10.1007/s12665-015-5115-y

ORIGINAL ARTICLE

Characteristics of water chemistry and its indication of chemical weathering in Jinshajiang, Lancangjiang and Nujiang drainage basins

Li-Li Zhang[1,2] · Zhi-Qi Zhao[1] · Wei Zhang[1,3] · Zheng-Hua Tao[1,2] · Lu Huang[1,2] · Jun-Xiong Yang[1,2] · Qi-Xin Wu[1] · Cong-Qiang Liu[1]

Received: 22 March 2015 / Accepted: 18 December 2015 / Published online: 16 March 2016

Abstract We present major ion compositions for water samples from Jinshajiang, Lancangjiang, and Nujiang drainage basins of China, collected in a water-rich period. This was done to determine natural chemical weathering rates on the eastern Himalayan and Qinghai-Tibet Plateau (HQTP), where anthropogenic impacts are considered small. The major ion distribution of the mainstream samples primarily reflects the weathering of carbonates, which accounts for ~46 % of total cations in the samples of Lancangjiang and Nujiang. Evaporite dissolution prevailed in the mainstream samples of Jinshajiang, as evidenced by high total dissolved solids (TDS) (364–479 mg/L) and Cl, SO_4, and Na-dominant major element composition. Silicate weathering contributed <16 % of total cations TDS in the studied rivers. Some samples of the Nujiang near the Tengchong Volcano showed distinctive silicate weathering signatures. Chemical erosion rates of carbonate were 22.5 and 42.7 t km^{-2} a^{-1} at Lancangjiang and Nujiang, respectively. At Jinshajiang, evaporite dissolution was important, with a weathering rate 29.5 t km^{-2} a^{-1}. The contributions of silicate weathering to total dissolved materials were minor, with weathering rates of 1.8, 2.2, and 5.1 t km^{-2} a^{-1} at Jinshajiang, Lancangjiang, and Nujiang, respectively. Net CO_2 consumption by silicate weathering was 96 × 10^3 mol km^{-2} a^{-1} on average, which is much less than values of the Indus, Ganges, and Brahmaputra draining the HQTP front, and the Amazon and Orinoco draining the Andes Mountains. However, total chemical denudation fluxes (including silicate, carbonate, and evaporite weathering) of the three rivers varied between 44.5 and 70.4 t km^{-2} a^{-1}, higher than published global mean values. This may indicate more intense chemical denudation for the three rivers draining the HQTP than those in the other areas of the world.

Keywords Jinshajiang · Lancangjiang · Nujiang · Water chemistry · Chemical weathering

✉ Zhi-Qi Zhao
zhaozhiqi@vip.skleg.cn

✉ Wei Zhang
zhangwei8086@163.com

[1] State Key Laboratory of Environmental Geochemistry, Institute of Geochemistry, Chinese Academy of Sciences, Linchengxi Road No. 99, Guanshanhu District, Guiyang 550081, China

[2] University of Chinese Academy of Sciences, Beijing 100049, China

[3] School of Geography and Tourism, Guizhou Normal College, Gaoxin Road No. 115, Wudang District, Guiyang 550018, China

Introduction

The Himalayan and Qinghai-Tibet Plateau (HQTP) is called the "Water Tower of Asia," because it is the source of the ten largest rivers in Asia, which are the water sources for ~40 % of global population (Huang et al. 2009). The Jinshajiang, Lancangjiang (Mekong), and Nujiang (Salween) regions (Three Rivers Region, TR R) make up a tectonically active region at the eastern margin of the HQTP (Hallet and Molnar 2001). Collision of the Indian and Eurasian plates led to several left-lateral strike-slip faults in the eastern HQTP, which produces extensional pull-apart basins and three steep valleys forming the TRR (Tapponnier et al. 1982; Holt et al. 1991; Wang and Burchfiel 2000). Topographic map or satellite images of the eastern HQTP reveals that the Jinshajiang, Lancangjiang and Nujiang run very close to each other, near the eastern Himalayan syntaxis

through three steep narrow ravines in the upper and middle parts of the river system (Hallet and Molnar 2001). We investigate the effect of this unusual geomorphology and strong topographic relief on water chemistry composition and chemical weathering processes of the three rivers.

Studying chemical weathering processes in the TRR is meaningful because the "tectonics-weathering-climate" hypothesis suggests uplift of the HQTP as a major driver of Cenozoic cooling because it caused increases in chemical weathering ability of silicates and thereby enhanced CO_2 drawdown from the atmosphere (Raymo and Ruddiman 1992). To test this hypothesis, rivers draining the HQTP have received considerable attention in recent years (e.g,. Gaillardet et al. 1999; Galy and France-Lanord 1999, 2001; Krishnaswami et al. 1999; Karim and Veizer 2000; Dalai et al. 2002; Oliver et al. 2003; Bickle et al. 2005; Singh et al. 2005; Moon et al. 2007; Hren et al. 2007; Wang et al. 2007; Wu et al. 2008; Noh et al. 2009; Jiang et al. 2015).

Geochemical data from the Ganges, Brahmaputra, and Indus originating on the southern flank of the Himalayas reveal that drainage basins of these rivers have greater chemical weathering rates than the average of the entire continent (e.g., Edmond 1992; Pande et al. 1994; Galy and France-Lanord 1999; Krishnaswami et al. 1999; Karim and Veizer 2000; Dalai et al. 2002; Bickle et al. 2003, 2005; Singh et al. 2005). Geochemical study on the upper Huang River indicates that silicate weathering and associated net CO_2 consumption rates of the northeastern HQTP were lower than the Ganges–Brahmaputra (Wu et al. 2005). Qin et al. (2006) examined fluvial geochemistry of the Min River, one of the headwater tributaries of the Changjiang River (Yangtze). They concluded that carbonate weathering was important and had higher chemical weathering rate in the Min River basin than the average of the Changjiang basin. The drainage area of the above rivers draining the HQTP represents a small portion of the entire HQTP. Wu et al. (2008) studied chemical weathering of seven major rivers (Jinshajiang, Lancangjiang, Nujiang, Yalong River, Min River, Dadu River, and upper Huang River) draining the eastern HQTP. These seven rivers have much larger drainage area than that of the Ganges, Brahmaputra, and Indus draining the southern flank of HQTP. The results of that study demonstrated that silicate weathering rates are generally lower than in rivers draining the Himalayan front. Similar conclusions were obtained by a chemical weathering study of the TRR by Noh et al. (2009). They compared three rivers to other rivers originating on the HQTP and non-HQTP rivers draining major orogenic zones of the world, showing that chemical weathering and CO_2 consumption rates of the three rivers were not significantly higher than those of other major rivers draining the Himalayan front and orogenic zones of the world.

Wu et al. (2008) selected only one sampling site, where each of the three aforementioned rivers flows down the plateau. Considering the potential effects of varying topography and geomorphology on water chemistry, data from one sampling site in each river may not be adequate to estimate chemical weathering in the entire drainage basins of the three rivers. Noh et al. (2009) estimated silicate weathering and CO_2 consumption rates of the TRR. However, they collected some samples in lower reaches of the TRR, where the rivers flow through heavily populated plains and hence may be polluted by industrialized and agricultural activities. Therefore, the estimated chemical weathering may be inadequate because of considerable anthropogenic impacts. The authors did not estimate carbonate and evaporite weathering and corresponding CO_2 consumption rates in the TRR. In the present study, we collected mainstream and tributary samples in the upper and middle reaches of the three rivers (Figs. 1, 2). The sampling areas have essentially no anthropogenic

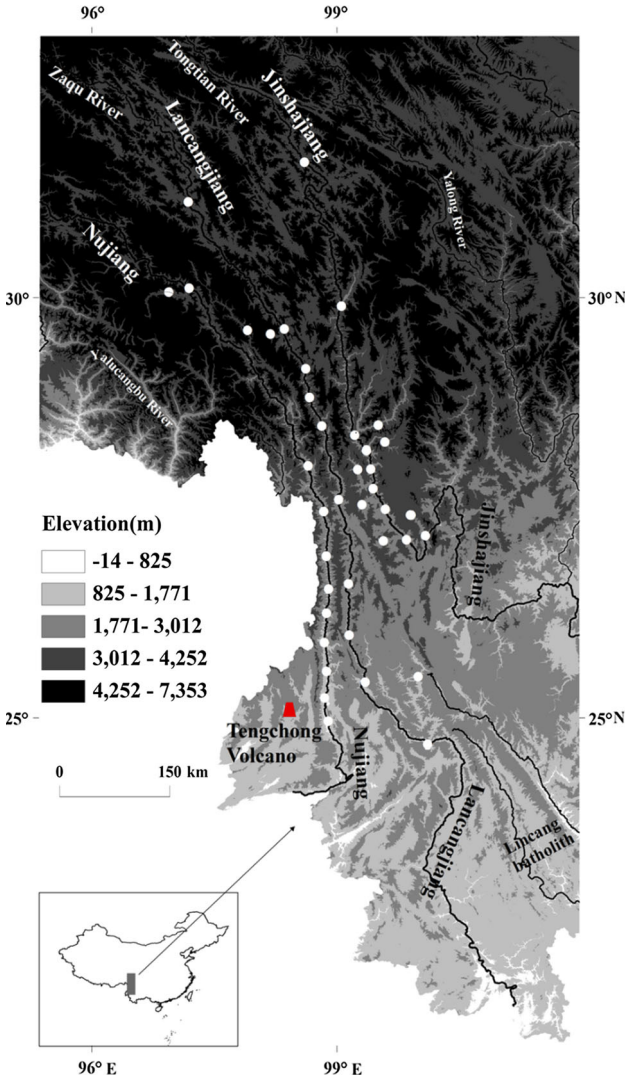

Fig. 1 Elevation map of the TRR in eastern HQTP, with sample locations and major rivers

pollution. Major elemental compositions of the water samples were analyzed to estimate chemical weathering and CO_2 consumption rates. We compared the three rivers to the results of Wu et al. (2008) and Noh et al. (2009), other rivers draining the HQTP, and rivers draining major orogenic zones of the world. Our study was aimed at in-depth understanding of major ion compositions and chemical weathering processes in the three river regions.

Study areas

The three rivers originate on the eastern margin of the HQTP and run towards the East China, South China, and Andaman seas, respectively. We mainly studied the upper and middle reaches of the rivers from their origin to their divergence in southwestern China (Fig. 1). The lithology of the studied basins was confirmed by the Geological Map of China (China Geological Survey 2004).

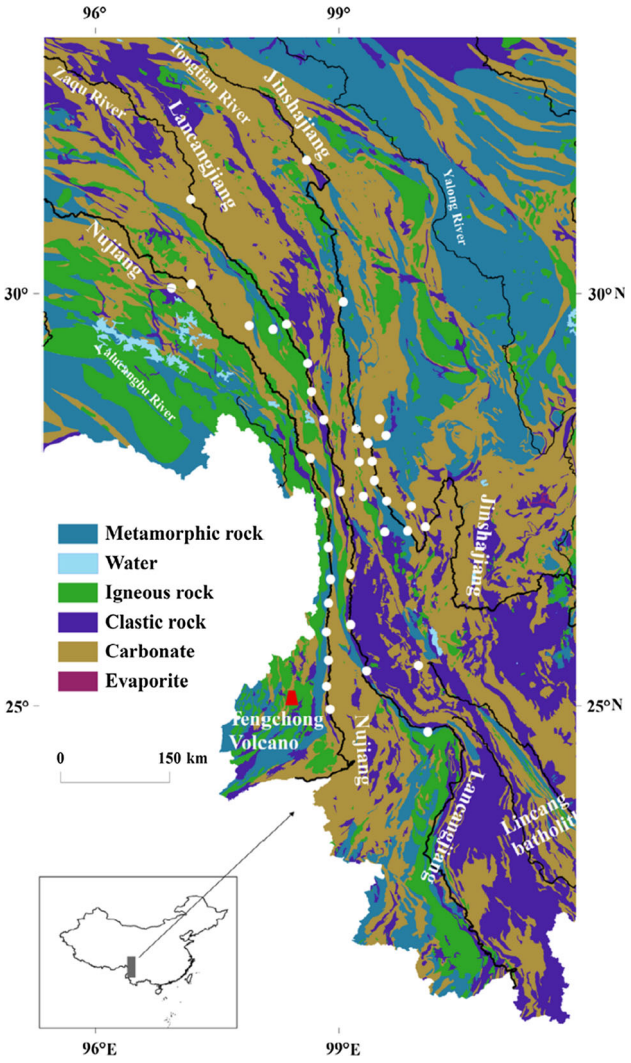

Fig. 2 Lithologic map of the TRR in eastern HQTP, with sample locations and major rivers. Lithology of the drainage basin is modified from the Geological Map of China (1:2,500,000, China Geological Survey 2004)

The Jinshajiang

As the headwater of the Changjiang River, the Jinshajiang has a length of ~2300 km. The drainage basin of Jinshajiang extends from 35°38′N 90°33′E to 25°97′N 104°64′E, with a total drainage area of 473,640 km^2. The source of the Jinshajiang is the Tuotuo River, originating on the eastern side of the Tanggula Mountains, the main peak of Geladandong Snow Mountain at an elevation of 6621 m. From the source area of the Jinshajiang Basin to where it reaches the fluvial plain (average elevation ~500 m) of the Sichuan Basin after flowing down the plateau, the population density is low. The study area of the Jinshajiang Basin is composed mainly of carbonates, Paleozotic clastic rocks, igneous rocks (mainly granitoid intrusive, and volcanic), lower-grade metamorphic rocks, and evaporite-bearing Quaternary deposits (Fig. 2). Ophiolite mélanges within the suture zones of Jinshajiang largely consist of basic and ultrabasic rocks and limestones (Wang et al. 2000).

The Lancangjiang

The Lancangjiang drainage basin extends from 33°81′N 94°40′E to 21°75′N 101°15′E, with a total length of ~2160 km and a drainage area of 167,400 km^2 in China. The Lancangjiang basin is sourced from rivers of Zaqu and Angqu, both rivers originate on the northern flank of the Tanggula Mountains. Below the source area, the Lancangjiang basin shows the main topographic features of high mountains, deep valleys and great changes of elevation, and has a very sparse population. In the lower reach, the Lancangjiang basin has less topographic changes and numbers of tributary increase. A famous tourist district called Xishuangbanna Dai Autonomous Prefecture is in the lower reach, in China's Yunnan Province, and has a dense population. The study area is composed mainly of Paleozotic clastic rocks, carbonates, low-grade metamorphic rocks, and volcanic rocks with some metamorphic and plutonic rocks (Fig. 2).

The Nujiang

The Nujiang drainage basin extends from 33°30′N 91°52′E to 24°11′N 99°17′E, with an area of 136,000 km^2 and a total length of ~2010 km in China. The source of Nujiang basin is the Naqu River, which originates on the southern flank of the Tanggula Mountains. Most of the Nujiang Basin in China is near the Lancangjiang. In the upper

reach, the Nujiang basin has a relatively flat topography. In the middle reach of the river, most of the mountains on the two sides of Nujiang have elevations of ~5000 m. The Nujiang flows through orogenic belts, where the deeply cutting Gaoligong Mountain, Biluo Snow Mountain, and Nu Mountain of the Traverse Range form a great gorge district. The elevation rapidly declines after the river flows across the Traverse Range. From the source area to near the end of that range, the population density is very low. The studied basin largely consists of carbonates, Paleozotic clastic rocks, low-grade metamorphic rocks, volcanic rocks (basaltic volcanic and granitoid intrusive), and Precambrian high-grade metamorphic rocks (Fig. 2).

Overall, carbonates make up ~63 %, igneous rock ~13 %, clastic rock ~12 %, metamorphic rock ~9 %, and evaporite ~3 % of the lithologic compositions in the studied basins (Fig. 2). The Lincang Batholith, a large body of plutonic acid rock (mostly Paleozoic granites), is found in the area of lower Lancangjiang and Nujiang next to the Changning-Menglian Ophiolite Belt (Wu et al. 1995). The Tengchong Volcano (25°19′N, 98°28′E), which erupted in the year 1609, is near the last sampling site in Nujiang basin (Figs. 1, 2).

Climate, vegetation, and population

Annual mean air temperature of the TRR ranges from −7 to 16 °C, with an average of ~1 °C. The studied basins are influenced by the Asian monsoon, which brings heavy rainfall in summer. Mean annual precipitation in the TRR is ~560 mm, more than 60 % of which falls in summer (Noh et al. 2009). Drainage basins in the HQTP interior are very arid, with a mean annual potential evapotranspiration of 684 mm (Burbank et al. 2003; Noh et al. 2009). Mean annual runoff increases gradually downstream, with ~245 mm above 4000 m elevation and 600 mm below that elevation (Noh et al. 2009). Alpine steppe mixed with grassland is the dominant vegetation in areas above 4000 m elevation. In downstream areas, the dominant vegetation is alpine scrub meadow, mixed coniferous forest, and subtropical forest. Local people build the terraced fields on the steep slopes and potatoes, corn, beans and rice are cultivated depending on elevation of the slope (Weyerhaeuser et al. 2005). The TRR has an average population density of 29 km^{-2}, which is low compared with the rest of China (Tian et al. 2006).

Sampling and analytical methods

Sampling

Discharge of the three rivers is greatly variable, seasonally and interannually. Time-series analyses of dissolved major element compositions at the Min River monitoring station showed that chemical weathering flux calculated using major ionic data during abundant water periods has the strongest agreement with annual time-series estimates (<±10 %) and poorest during water-scarce periods (up to 37 %) (Qin et al. 2006). Thus, we collected water samples in July and August 2013, corresponding to a water period (Table 1). Nine mainstream and six tributary samples were collected from the Jinshajiang Basin (Fig. 3), with an elevation ranging from >4200 to ~1200 m (Fig. 1). In Lancangjiang Basin, ten mainstream and three tributary samples were collected from upper-middle reaches (Fig. 3), with an elevation between 3863 and ~990 m (Fig. 1). Ten mainstreams and one tributary sample were collected in Nujiang Basin (Fig. 3). The elevation of sampling sites was between 2789 and ~688 m (Fig. 1). Between 15 and 20 L of river water was collected and filtered within 24 h of collection, using 0.45-μm cellulose acetate filters. The first liter was discarded and subsequent ones stored in acid-washed polyethylene bottles after filtering. Major cations were analyzed after acidification to pH 2 with ultrapure grade 1:1 nitric acid, and the filtered non-acidified samples were analyzed for major anions.

Analytical methods

pH and water temperature were measured in the field. Alkalinity was determined with the Gran titration method using 0.02 M HCl. Accuracies were ±0.01 in the determination of pH, ±0.1 (°C) for temperature, and ±0.01 (mL) for the amount of HCl consumed in the titration of alkalinity. Anions (Cl, SO_4, and NO_3) were measured by ionic chromatography with precision 5 %. Major cations (K, Na, Ca, and Mg) and silicic acid concentrations were determined by inductively coupled plasma optical emission spectrometry with precision better than 5 %. Reagent and procedural blanks were determined in parallel with sample treatment, and national standard reference materials of China (GBW(E)080118 for Ca, GBW(E)080126 for Mg, GBW(E)080127 for Na, GBW(E) 080125 for K, GBW(E)080272 for SiO_2, GBW(E)082048 for Cl, GBW(E)082050 for SO_4, and GBW(E)082049 for NO_3) were used in the determination of cations and anions.

Results and discussion

General characteristics of water chemistry

Data of pH, water temperature, major ions, silica, and total dissolved solids (TDS) in the rivers are presented in Table 1. pH of river water samples were neutral to mildly alkaline (7.53–8.70), and water temperatures were

Table 1 Dissolved major element concentrations for samples in the TRR

Sample ID	Rivers	Latitude	Longitude	Date (mm/dd/yy)	H (m)	pH	T (°C)	K (μM)	Na (μM)	Ca (μM)	Mg (μM)	Cl (μM)	NO_3 (μM)	SO_4 (μM)	HCO_3 (μM)	Si (μM)	TDS (mg/L)	TZ^+ (μEq)	TZ^- (μEq)	NICB (%)
J1	Jinshajiang mainstream	31°36.881′	98°36.051′	07/02/13	3031	8.42	15.8	74.0	3019	1185	750	2974	14.0	821	2520	108.1	479	6964	7149	−2.6
J2	Jinshajiang mainstream	29°53.904′	99°03.209′	07/02/13	2480	8.47	16.4	62.2	2276	1054	608	2174	17.6	603	2470	109.4	401	5663	5868	−3.5
J3	Jinshajiang mainstream	28°21.437′	99°12.870′	08/01/13	2189	8.33	16.8	50.6	1729	1119	567	1582	17.4	583	2654	137.7	379	5152	5419	−4.9
J4	Jinshajiang mainstream	28°11.042′	99°21.567′	08/01/13	2170	8.56	16.9	54.0	2408	1055	602	1999	14.3	757	2459	112.6	411	5776	5987	−3.5
J5	Jinshajiang mainstream	27°57.835″	99°24.746′	08/03/13	1932	8.61	16.9	50.8	1902	1044	581	1777	12.8	587	2470	117.2	375	5205	5434	−4.2
J6	Jinshajiang mainstream	27°43.750′	99°26.381′	08/03/13	1934	8.70	18.8	49.9	1867	1049	572	1734	15.3	566	2351	112.1	364	5158	5233	−1.4
J7	Jinshajiang mainstream	27°34.358′	99°32.664′	08/03/13	1898	8.73	17.5	49.3	1850	1025	564	1734	23.4	566	2622	117.8	379	5077	5511	−7.9
J8	Jinshajiang mainstream	27°07.273′	99°50.929′	08/03/13	1861	8.53	18.9	50.3	1868	1022	560	1754	17.9	562	2438	132.4	368	5081	5333	−4.7
J9	Jinshajiang mainstream	27°10.151′	100°04.200′	08/05/13	1895	8.43	17.6	46.7	1710	974	535	1627	15.4	537	2286	120.1	346	4774	5001	−4.5
JT10	Jinshajiang tributary (Shuoquhe)	26°47.736′	100°25.541′	08/03/13	2222	8.39	17.1	14.4	317	524	187	13.9	14.1	222	1528	119.4	152	1753	2000	−12.3
JT11	Jinshajiang tributary (Wensuihe)	26°11.635′	100°35.319′	08/03/13	1998	8.44	15.1	12.5	69.7	711	228	11.4	11.7	135	1733	93.4	158	1961	2027	−3.3
JT12	Jinshajiang tributary (Zibaluohe)	28°22.512′	99°14.324′	08/03/13	1919	8.21	15.1	8.7	47.3	434	81.1	10.6	13.0	50	867	88.1	82.0	1086	990	9.8
JT13	Jinshajiang tributary (Lapuhe)	28°09.719′	99°24.134′	08/04/13	1967	7.90	18.9	14.5	74.2	313	75.0	13.9	11.1	21	845	169.5	76.1	864	912	−5.2
JT14	Jinshajiang tributary (Zenlanhe)	27°46.508′	99°25.459′	08/04/13	1904	8.06	20.1	26.5	58.3	347	83.7	20.5	8.8	21	918	122.9	81.0	946	989	−4.3
JT15	Jinshajiang Tributary (Suoduohe)	27°34.877′	99°31.150′	08/04/13	1978	8.34	15.5	14.0	99.7	653	204	12.6	13.9	41	1679	102.1	144	1828	1789	2.2
L1	Lancangjiang mainstream	31°04.644′	97°11.960′	07/21/13	3233	8.44	13.7	36.3	492	1323	553	301	13.9	674	2600	81.2	316	4279	4263	0.4
L2	Lancangjiang mainstream	29°37.451′	98°21.169′	07/02/13	2668	8.41	16.5	24.0	580	1128	348	266	18.0	627	2373	78.8	285	3556	3911	−9.1
L3	Lancangjiang mainstream	28°58.779′	98°37.696′	07/31/13	2386	8.49	16.9	35.9	672	1212	536	266	10.5	726	2405	86.7	307	4204	4133	1.7
L4	Lancangjiang mainstream	28°50.877′	98°40.057′	07/31/13	2207	8.32	16.3	23.0	577	1105	439	265	9.6	613	2383	85.9	285	3688	3883	−5.0
L5	Lancangjiang mainstream	28°37.762′	98°44.129′	07/31/13	2120	8.33	16.4	26.3	566	1046	537	262	12.2	665	2416	87.0	283	3758	4020	−6.5
L6	Lancangjiang mainstream	27°40.437′	99°02.526′	08/01/13	1761	8.43	16.0	25.6	306	1069	497	239	17.4	569	2383	90.1	274	3463	3778	−8.3

Table 1 continued

Sample ID	Rivers	Latitude	Longitude	Date (mm/dd/yy)	*H* (m)	pH	*T* (°C)	K (μM)	Na (μM)	Ca (μM)	Mg (μM)	Cl (μM)	NO_3 (μM)	SO_4 (μM)	HCO_3 (μM)	Si (μM)	TDS (mg/L)	TZ^+ (μEq)	TZ^- (μEq)	NICB (%)
L7	Lancangjiang mainstream	26°20.224′	99°08.788′	08/01/13	1409	8.48	17.5	33.5	399	1047	476	230	14.6	547	2286	90.7	267	3479	3624	−4.0
L8	Lancangjiang mainstream	26°00.351′	99°08.636′	08/01/13	1350	8.38	18.0	33.7	524	1036	472	229	11.2	609	2297	91.2	276	3574	3754	−4.8
L9	Lancangjiang mainstream	25°25.608′	99°20.559′	08/01/13	1213	8.38	18.4	35.5	380	1000	439	220	15.2	504	2188	91.3	253	3292	3431	−4.1
L10	Lancangjiang mainstream	24°41.222′	100°05.875′	08/02/13	990	8.26	18.7	36.9	443	930	292	283	16.4	537	2134	106.4	251	2925	3509	−16.6
LT11	Lancangjiang tributary (Zongquhe)	29°33.940′	98°11.044′	08/02/13	3863	8.32	12.3	11.6	58.2	314	154	3.9	11.6	167	672	61.7	77.6	1005	1022	−2.1
LT12	Lancangjiang tributary (Shunbihe)	25°29.526′	99°58.974′	07/02/13	1309	8.29	19.8	41.3	232	707	240	108	13.9	135	1896	128.0	177	2169	2287	−5.2
LT13	Lancangjiang tributary (Yuquhe)	29°45.661′	97°43.185′	08/04/13	3875	8.35	19.3	17.9	96.9	526	252	3.3	9.0	93	1343	69.8	123	1671	1542	8.2
N1	Nujiang mainstream	30°05.288′	97°14.203′	07/21/13	2789	8.42	15.7	24.3	171	721	502	26.6	16.8	433	1712	79.5	196	2641	2620	0.8
N2	Nujiang mainstream	27°32.738′	98°49.663′	08/03/13	1366	8.28	17.7	29.0	177	731	484	26.7	10.4	430	1739	88.8	198	2636	2636	0.0
N3	Nujiang mainstream	27°14.295′	98°53.654′	08/03/13	1272	8.26	18.7	28.7	173	714	472	26.5	9.0	413	1658	92.1	190	2575	2520	2.2
N4	Nujiang mainstream	26°55.637′	98°52.101′	08/04/13	1201	8.27	20.2	29.7	171	715	462	26.2	8.9	405	1674	92.1	190	2554	2518	1.4
N5	Nujiang mainstream	26°32.176′	98°53.833′	08/04/13	1055	8.28	19.8	29.7	168	701	462	26.2	11.2	402	1625	86.6	186	2523	2466	2.3
N6	Nujiang mainstream	26°15.002′	98°52.208′	08/04/13	931	8.26	20.0	30.0	165	698	452	25.8	7.7	394	1625	89.8	185	2496	2447	2.0
N7	Nujiang mainstream	25°53.991′	98°50.620′	08/04/13	844	8.23	20.0	31.0	163	688	446	24.5	13.3	381	1658	85.6	185	2463	2458	0.2
N8	Nujiang mainstream	25°33.283′	98°52.216′	08/04/13	749	8.25	19.5	30.6	171	702	455	26.5	5.6	380	1658	99.5	186	2516	2450	2.7
N9	Nujiang mainstream	25°14.393′	98°50.881′	08/05/13	700	8.15	21.2	29.8	164	689	443	25.6	14.8	275	1609	93.8	182	2460	2199	11.8
N10	Nujiang mainstream	25°56.041′	98°53.218′	08/05/13	688	8.13	20.8	30.5	160	594	405	25.8	17.2	246	1459	97.4	165	2188	1994	9.8
NT11	Nujiang tributary (Lengquhe)	30°03.958′	97°09.452′	08/05/13	2849	8.36	12.5	22.0	133	493	170	16.5	10.9	235	845	76.3	105	1481	1343	10.3

H elevation of sampling sites, *TDS* total dissolved solids, *NICB* normalized inorganic charge balance = $(TZ^+ - TZ^-)/TZ^+ \times 100$ %

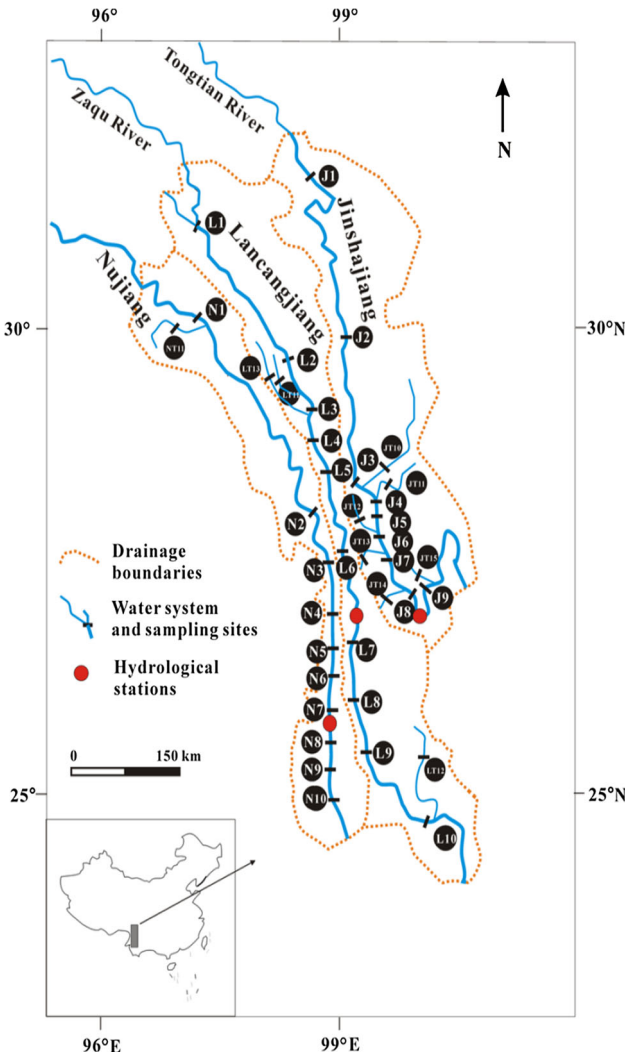

Fig. 3 Sampling location map for 39 river water samples in the TRR. Dashed lines mark drainage area divides of the three rivers

8.9–22.7 °C (Table 1). The pH values obtained in TRR water suggest that alkalinity is imparted primarily by bicarbonates, reflecting the intensity of water–rock interactions and weathering of carbonates. The temperature of river water reflects the elevations of the sampling sites.

Total cationic charge ($TZ^+ = K + Na + 2Ca + 2 Mg$), as a measure of total dissolved content, was strongly variable, from 2188 to 6964 μEq L^{-1} in mainstream samples of the studied rivers (Table 1). This was within the range measured in the 61 largest rivers of the world (Gaillardet et al. 1999). The mean value of 3797 μEq L^{-1} was much larger than the estimated average of world rivers ($TZ^+ = 1125$ μEq/L, Meybeck 2003), and larger than values of the Min River ($TZ^+ = 1300$–4100 μEq L^{-1}, Qin et al. 2006), Yalong River ($TZ^+ = 225$–3974 μEq L^{-1}, Li et al. 2014), Jialingjiang ($TZ^+ = 3708$ μEq L^{-1}, Li et al. 2011) and upper Xijiang ($TZ^+ = 3456$ μEq L^{-1}, Xu and Liu 2007), but smaller than a value reported for Wujiang River, which drains karst terrain ($TZ^+ = 4140$ μEq L^{-1}, Han and Liu 2004). The first two rivers and the studied rivers are all on the eastern HQTP and the last three rivers are in southwestern China.

The extent of TZ^+–TZ^- charge imbalance, characterized in terms of normalized inorganic charge balance (NICB = $(TZ^+–TZ^-)/TZ^+ \times 100$ %, where $TZ^- = HCO_3 + Cl + NO_3 + 2SO_4$ in μEq), was generally within ±10 % for most samples, indicating that TZ^+ is balanced by the total anionic charge (TZ^-) and that unanalyzed organic anions are only a minor component. As indicated in Table 1 and Figs. 1 and 2, samples with TZ^+ >4000 μEq L^{-1} were from the Jinshajiang mainstream, and they show input from evaporite dissolution (high Na and $Cl + SO_4$). Samples with TZ^+ between 1000 and 4000 μEq L^{-1} were from Lancangjiang and Nujiang samples, showing dominant input from carbonate weathering.

TDS (mg L^{-1}), expressed here as the sum of major inorganic species concentrations ($Na + K + Ca + Mg + HCO_3 + Cl + SO_4 + NO_3 + SiO_2$) of mainstream samples of the TRR, decreased from 196–479 mg L^{-1} above 2000 m elevation to 165–379 mg L^{-1} downstream, owing to dilution. There was a strong correlation between TDS and TZ^+ ($r^2 = 0.98$, $n = 39$) for all samples.

Major ion distributions

Ternary diagrams of dissolved major elements effectively show a wide diversity of composition of all samples collected in the drainage basins (Fig. 4), which attests to the presence of diverse lithological components within the study area. As shown in anion ternary diagrams (Fig. 4a), most of the data concentrate near the HCO_3 apex and lie along the HCO_3–($SO_4 + Cl$) line, characteristic of carbonate–evaporite–sulfide weathering.

HCO_3 is the dominant anion, ranging from 671 to 2520 μmol L^{-1} with a mean 1535 μmol L^{-1} for all water samples, constituting on average 64, 73, and 72 % of the anion budget in Jinshajiang, Lancangjiang, and Nujiang, respectively. Cl and SO_4 are also important anions, accounting for >22 % of total anion composition in the three rivers. In tributary samples, the greatest HCO_3 was observed in samples JT15 (1679 μmol L^{-1}) and LT12 (1896 μmol L^{-1}), and most HCO_3 was basically balanced by Ca and Mg in the two samples [$(Ca + Mg)/HCO_3 = 0.51$ and 0.49 for JT15 and LT12, respectively.]

On the cation ternary diagram (Fig. 4b), most of the samples cluster near the Ca apex and lie along the Ca–Mg line. Cationic composition of river water samples were mostly dominated by Ca, with the order Ca > Mg > Na > K. The concentration of Ca was 313–1185 μmol L^{-1}

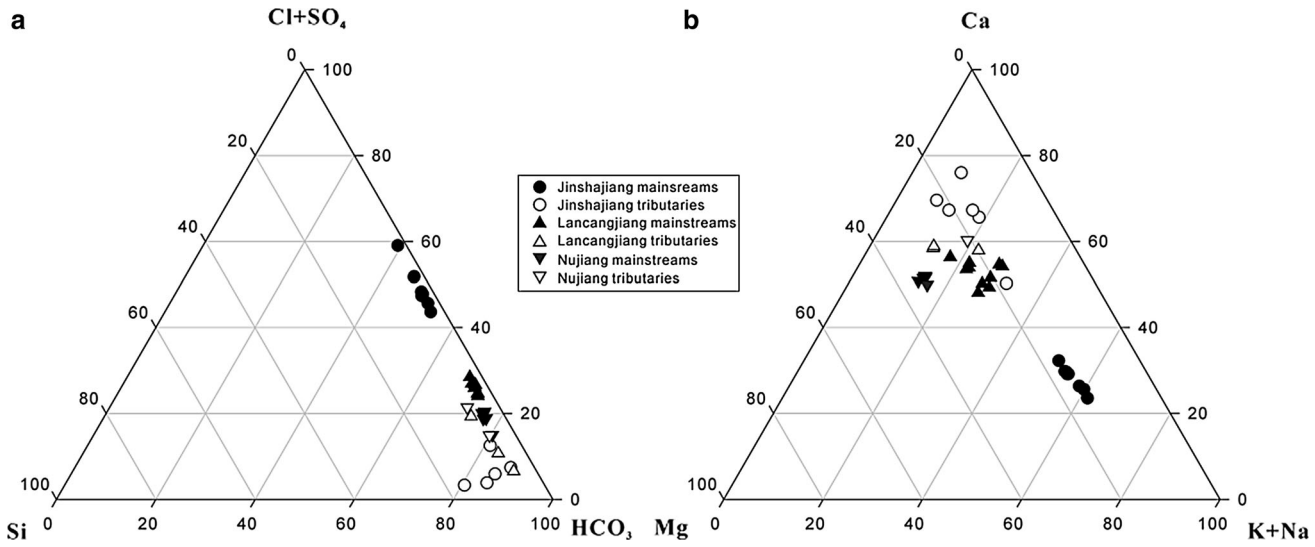

Fig. 4 Ternary diagrams showing anion-Si compositions (**a**) and cations (**b**)

in the three rivers, with averages of 807, 957, and 676 μmol L^{-1} for Jinshajiang, Lancangjiang, and Nujiang, respectively. The concentration of Mg varied between 75 and 750 μmol L^{-1}, accounting for more than 15 % (in μmol L^{-1}) of total cation concentrations in river waters. Ca and Mg constituted >80 % of total cation concentrations in most of the samples. Na was the third most abundant cation, ranging from 58 to 672 μmol L^{-1}, except for the Jinshajiang mainstream samples, representing >9 % in most of the river waters. The K concentration was relatively low over the entire basin, and is estimated to be ~3 % of total cation composition.

All these results generally demonstrate the dominance of carbonate weathering in the study basins. In the samples, significant correlation was observed between HCO_3 and Ca ($r^2 = 0.92$, $n = 30$). An exception to this general ion distribution is Cl-, SO_4-, and Na-dominant samples from the Jinshajiang mainstream. As seen in the ternary ion diagrams (Fig. 4), data points of those samples are more similar to the Cl + SO_4 apex and K + Na apex. In these samples, Cl (in μmol L^{-1}) makes up >36 % and SO_4 >11 % of the total anion budget, and Na^+ forms >52 % of the total cation budget. Fu et al. (1998) and Zhao et al. (2003) showed that the Chumar and Tuotuo Rivers, the two main tributaries of the Jinshajiang, have extremely high concentrations of Na and Cl (~10,000 μmol L^{-1}), which is mainly attributed to weathering and dissolution of halite (Bureau of Geology and Mineral Resources of Qinghai Province 1990) and the contribution from saline lakes and hot springs in the drainage areas (Shui et al. 2006a, b). The Cl-, SO_4-, and Na-dominant ion compositions may derive from extreme headwater tributaries in the source areas of the Jinshajiang. In the samples, significant correlation was observed between Na and Cl ($r^2 = 0.94$, $n = 9$).

Figure 5 shows the equivalent charge balance of Ca + Mg vs. HCO_3 and vs. HCO_3 + SO_4, plus Ca + Na vs. HCO_3 + Cl. In the tributary samples of the Jinshajiang, Lancangjiang, and Nujiang, HCO_3 is basically balanced by Ca + Mg, and SO_4 is not significant in the chemical equilibrium (Fig. 5a). However, for the mainstream samples of the three rivers, Ca + Mg was greater than HCO_3 but smaller than HCO_3 + SO_4 (Fig. 5b), indicating measurable contribution from the dissolution of evaporite minerals (gypsum-salt layer) or oxidation of sulfide minerals such as pyrite (FeS_2). The best correlation was between Ca + Na and HCO_3 + Cl ($r^2 = 0.98$, $n = 39$) (Fig. 5c), and the data points were mostly on the [Ca + Na]:[HCO_3 + Cl] = 1:1 line, indicating that HCO_3 + Cl was well balanced by Ca + Na. This observation suggests that halite (NaCl) dissolution in addition to carbonate weathering and evaporite (mainly gypsum) dissolution is important in the equivalent charge balance of most river waters.

Sources of major ions in rivers

Dissolved ions in river water result from atmospheric inputs, anthropogenic inputs, weathering of silicate, carbonate and evaporates, and oxidation of sulfide minerals. Thus, for any element X in river water, the budget equation can be written as

$$[X]_{river} = [X]_{rain} + [X]_{anthropogenic} + [X]_{carb} + [X]_{sil} + [X]_{evap} + [X]_{sulfide}, \quad (1)$$

where subscripts "carb", "sil", and "evap" represent inputs from weathering of carbonate, silicate, and evaporite, respectively. It is necessary to constrain the

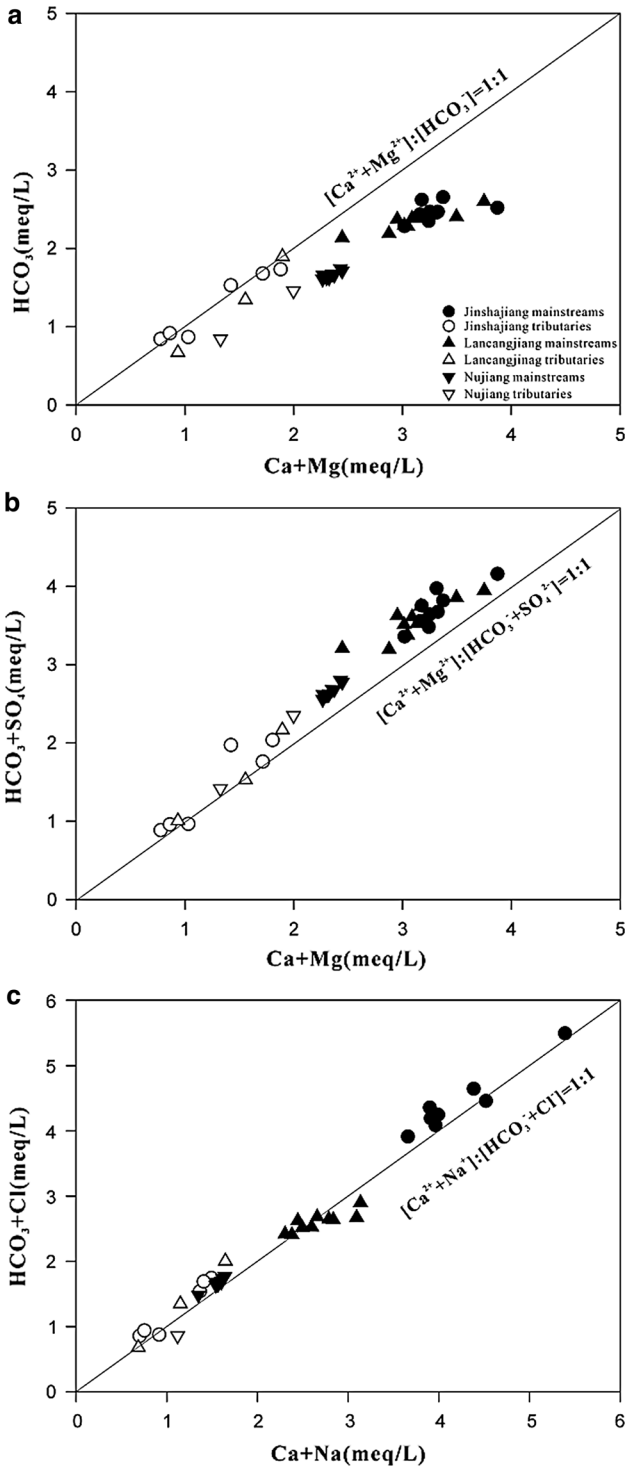

Fig. 5 Equivalent charge balance of [Ca + Mg] vs. HCO_3 (**a**), [Ca + Mg] vs. [HCO_3 + SO_4] (**b**), and [Ca + Na] vs. [HCO_3 + Cl] (**c**)

contributions from these sources to the dissolved load to derive chemical weathering rates and associated CO_2 consumption within the basin.

Atmospheric inputs and anthropogenic contributions

Atmospheric input is typically considered to enhance the chemical composition of riverine water. To examine the lithologic origin of the dissolved load, one must first correct for that input. As shown by numerous research works, Cl, whose concentration is generally very low in carbonate and silicate rock, is the most commonly used element to evaluate the atmospheric contribution to the chemical composition of river water (Negrel et al. 1993; Xu and Liu 2007; Liu et al. 2013).

To determine atmospheric Cl inputs to the three rivers, we considered rivers that do not drain any saline formation or hydrothermal area (Rai et al. 2010). Lancangjiang tributary sample LT13 (collected at Yuquhe) had the lowest Cl concentration of 3.3 μmol L^{-1} (Table 1), and no salt-bearing rocks or hydrothermal areas were found by field observation and via knowledge of the river basin geology. We assumed that the sample of lowest Cl concentration (LT13, 3.3 μmol L^{-1}) acquired its dissolved Cl exclusively from rain. The atmospheric contribution of element X (X = Ca, Mg, Na, K, and SO_4) to river water can be derived from

$$[X]_{rain} = [Cl]_{rain} \times [X/Cl]_{rain}, \quad (2)$$

where $[X]_{rain}$ is the contribution of element X from rain (μmol L^{-1}) to rivers; $[Cl]_{rain}$ (=3.3 μmol L^{-1}) is the atmospheric contribution of Cl to river water; and $(X/Cl)_{rain}$ is the molar ratio of element X over Cl in rainwater. X/Cl ratios in precipitation at three Tibetan towns that were volume-weighted means over 1998–2000 were used as $(X/Cl)_{rain}$ in the calculation (Zhang et al. 2003). These were Na/Cl = 4.17, Mg/Cl = 1.79, Ca/Cl = 16.06, K/Cl = 3.55, and SO_4/Cl = 1.03. Rain percentages were calculated by dividing the sum of the cations from rain ($\sum cation_{rain} = Na_{rain} + K_{rain} + Ca_{rain} + Mg_{rain}$ = 49.1 - μmol L^{-1}) by $(\sum cation)_{river}$.

Most of the sampling sites in the upper reaches of the Jinshajiang, Lancangjiang, and Nujiang are unaffected by industrial and agricultural activities and are far from densely populated areas (some areas are basically pristine). Direct anthropogenic contributions to their major ion budgets are consequently small. River nitrate concentrations, which are often used as an indicator of anthropogenic activities, were low (Table 1). Therefore, direct anthropogenic contamination is negligible.

Evaporite dissolution

According to the estimate of Meybeck (1987), the dissolution rate of evaporite is 40–80 times that of granites, and 4–7 times that of carbonate. Consequently, evaporite dissolution can significantly influence river chemistry, even if

evaporite outcrops are sparse in a basin. Noh et al. (2009) showed that evaporite (halite plus gypsum/anhydrite) dissolution is important in the dissolved load of water samples in the three rivers.

In the present study, we estimated the contributions from evaporite (chloride and sulfate salts) after a rain correction. Assuming all Cl in river water remaining after that correction comes from halite ($Cl_{evap} = Cl_{river} - Cl_{rain}$; $Na_{evap} = Cl_{evap}$) and all SO_4 from gypsum/anhydrite ($SO_{4evap} = SO_{4river} - SO_{4rain}$; $Ca_{evap} = SO_{4evap}$), we approximated the contribution to riverine cations from halite ($Cl_{evap}/\sum cation_{river}$) and sulfate ($SO_{4evap}/\sum cation_{river}$) dissolution.

Silicate weathering

For cations, silicate weathering input to the dissolved Na and K mainly from aluminosilicate weathering and Ca and Mg mainly from calcium-magnesium silicate weathering in river water (Wu et al. 2008). We assumed that all Na remaining after rain and halite correction is silicate derived ($Na_{sil} = Na_{river} - Na_{rain} - Na_{evap}$) and that all dissolved K in the river after rain correction is from silicate ($K_{sil} = K_{river} - K_{rain}$).

The ratio $Si/(Na_{sil} + K_{sil})$ is a proxy commonly related to the ''intensity'' of silicate weathering (Edmond et al. 1995). Here, Si represents the content of dissolved silicon, mainly originating from silicate weathering, and Na_{sil} and K_{sil} represent the contents of Na and K from silicate weathering in the rivers. $Si/(Na_{sil} + K_{sil}) = 1.7$ for weathering of average shield to kaolinite and 3.5 to gibbsite, and 1.0 for average shale to kaolinite and 3.4 to gibbsite (Huh et al. 1998). Most of the $Si/(Na_{sil} + K_{sil})$ ratios were <1.7 (Fig. 6), indicating that silicate weathering in the Jinshajiang, Lancangjiang, and Nujiang basins is superficial, i.e., to cation-rich secondary minerals but not to kaolinite or gibbsite.

The contribution of Na in the rivers from carbonate weathering may be neglected (Dalai et al. 2002). On average, Na_{sil} and K_{sil} together constitute only ~22 % of total cations in most river waters, suggesting that silicate weathering is not a major source of cations for the rivers at basin scale. Considering that there are other sources of Na such as borax, mirabilite, or trona in the evaporite deposits of the three river basins, correction for evaporites and rain using Cl_{evap} and Na_{rain} as indices can give an upper limit of Na from silicates.

Ca in river waters is mainly derived from carbonates, evaporites, and silicates, whereas sources for Mg are carbonates and silicates. In river waters, Ca and Mg derived from silicate weathering (Ca_{sil} and Mg_{sil}) can be obtained from Na_{sil} and K_{sil} using appropriate $(Ca/Na)_{sil}$ and $(Mg/K)_{sil}$ molar ratios (Galy and France-Lanord 1999). The

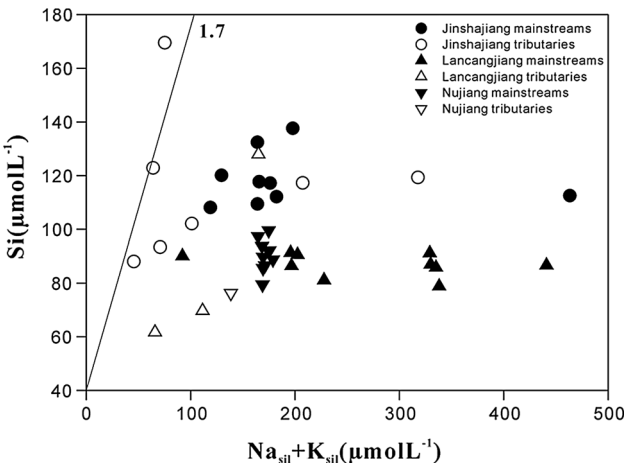

Fig. 6 Relationship between Si and $(Na_{sil} + K_{sil})$

reliabilities of $(Ca/Na)_{sil}$ and $(Mg/K)_{sil}$ directly affect the proportion of dissolved cations resulting from silicate weathering, and this requires some care.

For estimating the silicate contributions of Ca and Mg to rivers in the Nepal Himalaya, values of 0.18–0.3 and 0.5 ± 0.2, respectively, for $(Ca/Na)_{sil}$ and $(Mg/K)_{sil}$ were used by Galy and France-Lanord (1999), which are based on (Ca/Na) in silicate composition of original rock in the Higher Himalaya (HH) and Lesser Himalaya (LH) and in plagioclase of the High Himalaya Crystalline (HHC). Based on (Ca/Na) in LH granites/gneisses, soil profiles, and rivers draining predominately silicates, Krishnaswami et al. (1999) used the values 0.7 ± 0.3 and 0.3 ± 0.2, respectively, for $(Ca/Na)_{sil}$ and $(Mg/Na)_{sil}$. Dalai et al. (2002) used two values (0.7 ± 0.3 and 0.35 ± 0.15) for $(Ca/Na)_{sil}$ for estimation of Ca_{sil} in the Yamuna Basin. Values of 0.7 and 0.3, respectively, for (Ca/Na) and (Mg/Na) in the silicate fraction in the Min River basin were used by Qin et al. (2006). $(Ca/Na)_{sil} = 0.2$ and $(Mg/Na)_{sil} = 0.5$ were used for the Wujiang and upper Xijiang basins (Xu and Liu 2007; Han and Liu 2004). Moon et al. (2007) assumed a Ca/Na of 0.44 and Mg/Na of 0.16 for silicate fraction in the Hong River drainage basin. Therefore, estimation of $(Ca/Na)_{sil}$ and $(Mg/K)_{sil}$ has considerable variability. For the large TRR, local bedrock has the wide variety ranging from acid plutonic rocks to basaltic ophiolite mélanges (Wang et al. 2000).

According to Blum et al. (1998), samples of riverbed sand can represent unweathered bedrock in the watershed. We used Ca/Na ratios measured in the silicate fraction of riverbed sediment as $(Ca/Na)_{sil}$, which was measured and used by Wu et al. (2008) in a calculation of cation contributions from silicate weathering to seven rivers draining the eastern HQTP. According to Wu et al., the $(Ca/Na)_{sil}$ molar ratio of the silicate fraction of riverbed sediments was 0.40, 0.17, and 0.29 for Jinshajiang, Lancangjiang, and

Nujiang, respectively. Similarly, the Mg contribution from silicate (Mg_{sil}) in rivers can also be obtained using river K_{sil} to multiply the $(Mg/K)_{sil}$ molar ratio of the silicate fraction of riverbed sediments (Blum et al. 1998). The latter ratio was 0.84 for Jinshajiang, 0.50 for Lancangjiang, and 0.42 for Nujiang (Wu et al. 2008). Our values of $(Ca/Na)_{sil}$ in the three rivers are similar to other drainage basins in the HQTP and a common set of ratios for global river silicate end member composition of 0.35 ± 0.15 (Gaillardet et al. 1999).

According to the above values, the fraction of cation contributions from the silicates to the three rivers could be calculated as in Dalai et al. (2002):

$$\left((\sum \text{cation})_{sil} = \frac{\sum (Xi)_{sil}}{(\sum \text{cation})_{river}} = \frac{(Na_{sil} + K_{sil} + 2 \times Ca_{sil} + 2 \times Mg_{sil})}{(Na_{river} + K_{river} + 2 \times Ca_{river} + 2 \times Mg_{river})} = \left(\frac{Na_{sil} + K_{sil} + 2 \times (Ca/Na)_{sil} \times Na_{sil} + 2 \times (Mg/K)_{sil} \times K_{sil}}{Na_{river} + K_{river} + 2 \times Ca_{river} + 2 \times Mg_{river}} \right) \right)$$

Here, Na_{river}, K_{river}, Ca_{river}, and Mg_{river} represent total contents of each element in river waters, whereas Na_{sil}, K_{sil}, Ca_{sil} and Mg_{sil} indicate elemental concentrations derived from the silicate fraction, and $(Ca/Na)_{sil}$ and $(Mg/K)_{sil}$ denote elemental molar ratios of silicate fraction in riverbed sediments.

Carbonate weathering

In many watersheds of the world, carbonate weathering is important in controlling river water chemistry, regardless of the major rock type or not in local area, because carbonate is more susceptible to weathering than silicate (Roy et al. 1999; Karim and Veizer 2000).

It has been observed during field work that carbonate rocks constitute a major lithology in the catchment basins of these rivers. HCO_3 and Ca are the major anion and cation in the three rivers. Furthermore, compared with most major rivers in the world (Gaillardet et al. 1999), the three river samples are characterized by higher alkalinity, implying that the contribution from carbonate weathering is significant.

Any remaining cations not accounted for by rain, evaporates, halites, and silicates are attributed to carbonate weathering. We calculated the contribution of carbonate weathering to riverine cations:

$$(\sum \text{cation})_{carb} = \frac{\sum (Xi)_{carb}}{(\sum \text{cation})_{river}} = \frac{(2 \times Ca_{carb} + 2 \times Mg_{carb})}{(Na_{river} + K_{river} + 2 \times Ca_{river} + 2 \times Mg_{river})} = \left(\frac{2 \times (Ca_{river} - Ca_{sil} - Ca_{eva} - Ca_{rain}) + 2 \times (Mg_{river} - Mg_{sil} - Mg_{rain})}{Na_{river} + K_{river} + 2 \times Ca_{river} + 2 \times Mg_{river}} \right)$$

Chemical budget and calculation results

To quantify the contributions from rain input, evaporite (halite and gypsum) dissolution, carbonate and silicate weathering, a forward model based on mass balance was used. For each element, we can write mass balance equations with the assumptions discussed above.

$$[Cl]_{rain} = 3.3 \mu mol/L \quad (3)$$

$$[Cl]_{river} = [Cl]_{rain} + [Cl]_{evap} \quad (4)$$

$$[SO_4]_{river} = [SO_4]_{rain} + [SO_4]_{evap} \quad (5)$$

$$[Na]_{river} = [Na]_{rain} + [Na]_{evap} + [Na]_{sil} \quad (6)$$

$$[K]_{river} = [K]_{rain} + [K]_{sil} \quad (7)$$

$$[Ca]_{river} = [Ca]_{rain} + [Ca]_{evap} + [Ca]_{carb} + [Ca]_{sil} \quad (8)$$

$$[Mg]_{river} = [Mg]_{rain} + [Mg]_{carb} + [Mg]_{sil} \quad (9)$$

$$Ca_{sil} = Na_{sil} \times (Ca/Na)_{sil} \quad (10)$$

$$Mg_{sil} = K_{sil} \times (Mg/K)_{sil} \quad (11)$$

The calculated contributions of various weathering sources to the cationic TDS (mg L^{-1}) for the TRR are illustrated in Fig. 7. Cationic TDS is equal to the sum of K, Na, Ca, and Mg from the different reservoirs.

Atmospheric inputs were generally minor in the TRR. Cations from atmospheric sources accounted for 0.9–3.9 % of total riverine cations in Jinshajiang, 1.9–2.8 % in Lancangjiang, and 3.3–4.1 % in Nujiang. However, in some small tributaries (samples JT12, JT13, JT14, and LT11) with low TDS (76.1–82.0 mg/L), rain can provide as much as $\sim$10 % of dissolved cations.

Assuming that evaporite is composed of halite and gypsum, cationic TDS contributions from halite and gypsum dissolution were calculated separately. Halite contributions were minor for most samples. Large halite proportions (39.7–49.8 %) were seen in the Jinshajiang mainstream samples. Substantial sulfate salt contributions of 25.5–37.8 and 33.0–38.5 % were calculated for the Nujiang and Lancangjiang mainstream samples, respectively. The exact mineralogy of the sulfate salt (e.g., $CaSO_4$, $MgSO_4$, and Na_2SO_4) does not affect the sulfate budget but can affect that of silicates and carbonates.

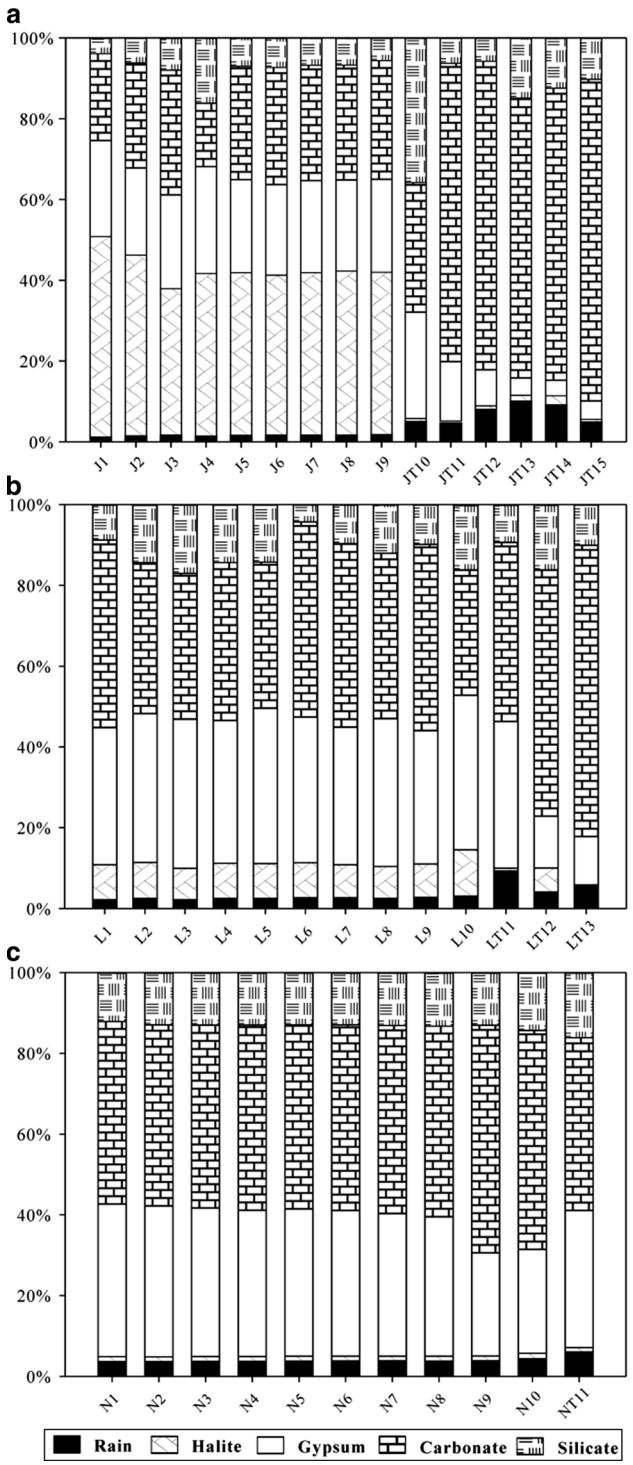

Fig. 7 Calculated contributions of various reservoirs to cationic TDS (mg L^{-1}) from the forward method for Jinshajiang (**a**), Lancangjiang (**b**), and Nujiang (**c**)

Sulfate is also likely generated by sulfide oxidation, and therefore this estimate is an upper limit of the gypsum contribution.

Silicate contributions of cations, $(\sum \text{cation})_{sil}$, in the studied rivers were generally <16 % (average 13 %) of total cations, except for one Jinshajiang tributary sample (JT10) at 35.8 % (Fig. 7). There are two sources of uncertainty in these estimates. The misallocation of sulfate salts to gypsum/anhydrite instead of Na-sulfate can overestimate Na_{sil} and hence $(\sum \text{cation})_{sil}$. The large $(\sum \text{cation})_{sil}$ calculated for JT10 is suspect because of the possible existence of Na_2SO_4. Additionally, considering uncertainties of ±50 % for $(Ca/Na)_{sil}$ and $(Mg/K)_{sil}$ molar ratios, the propagated error is 11.4–20.4 % in the $(\sum \text{cation})_{sil}$ calculations.

Furthermore, we did not observe any general correlations between cations derived from silicate weathering ($Cation_{sil} = Na_{sil} + K_{sil} + Ca_{sil} + Mg_{sil}$) and SiO_2 in any mainstream samples of the three rivers. Likewise, Wu et al. (2008) also found no general correlations between $Cation_{sil}$ and SiO_2 in the seven rivers draining the HQTP. Some possible reasons are: (1) The varying lithological formations, terrain, and topography may control the chemical weathering rate of the three river basins. (2) The abundant evaporite minerals in the three drainage basins and saline lakes near the source areas are rich in trona, soda, borax, epsomite, and mirabilite (Yu and Tang 1981), which can result in overestimation of the contribution of silicate weathering. (3) Many unevenly distributed thermokarst lakes are found in source areas of the Jinshajiang, Lancangjiang, and Nujiang basins (Frenzel et al. 1995). Some dissolved Si may be consumed by diatom growth in thermokarst lakes (Huh et al. 1998).

Carbonate weathering contributed 42.8–56.4, 36.4–48.3, and 15.8–39.2 % of total cations in mainstream samples of Nujiang, Lancangjiang, and Jinshajiang, respectively. High $(\sum \text{cation})_{carb}$, between 32.0 and 79.7 %, was found in the tributary samples of the three river basins. As mentioned for silicate contributions, the assumption of all sulfates being gypsum or anhydrite may underestimate Ca_{carb} and hence $(\sum \text{cation})_{carb}$. This is because sulfide oxidation can produce SO_4, although SO_4 concentrations are generally lower than Ca concentrations. Thus, the calculated $(\sum \text{cation})_{carb}$ is a lower limit of the carbonate contribution.

In summary, the result of the forward model showed that weathering of evaporite (halite and gypsum) followed by carbonate weathering is dominant in the Jinshajiang mainstream, and weathering of carbonate and gypsum is important in mainstream samples of Lancangjiang and Nujiang. Silicate weathering is not important as that of evaporite and carbonate in terms of cation contribution percentages. Carbonate weathering was the major contributor in the tributary samples of the TRR.

Table 2 Chemical weathering and CO_2 consumption rates for TRR draining the HQTP calculated by the forward model

Rivers	Discharge ($km^3\ a^{-1}$)	Drainage area (km^2)	SWR		$\Phi[CO_2]_{sil}$		CWR		$\Phi[CO_2]_{carb}$		EWR	References
			t $km^{-2}\ a^{-1}$	m ka^{-1}	CO_2 10^3 mol $km^{-2}\ a^{-1}$	CO_2 10^9 mol a^{-1}	t $km^{-2}\ a^{-1}$	mm ka^{-1}	CO_2 10^3 mol $km^{-2}\ a^{-1}$	CO_2 10^9 mol a^{-1}	t $km^{-2}\ a^{-1}$	
Jinshajiang	39.4	229,492	1.8	0.7	45.6	10.4	16.8	7.0	157.8	36.2	29.5	This study
Jingshajiang	39.4	233,000	9.1	3.4	370	86	11.5	4.8	130	29		Wu et al. (2008)
Changjiang	928	1,808,000	5.3	1.9	59.2	107	55.8	23.3	551.4	997	3.8	Gaillardet et al. (1999)
Lancangjiang	29.0	113,434	2.2	0.8	84.9	9.6	22.5	9.4	191.3	21.7	19.8	This study
Lancangjiang	29.0	89,000	4.1	1.5	70	6	50.1	20.9	520	46		Wu et al. (2008)
Mekong	467	325,000	6.3	2.3	107.3	194	24.5	10.2	226.2	409	9.4	Gaillardet et al. (1999)
Nujiang	53.1	85,865	5.1	1.9	157.5	13.5	42.7	17.8	450.5	38.7	22.6	This study
Nujiang	53.1	110,000	5.9	2.2	110	12	57.1	23.8	590	65		Wu et al. (2008)
Yalong River	55.3	129,000	8.0	3.0	240	31	36.1	15.0	380	49		Wu et al. (2008)
Dadu River	61.6	89,000	8.3	3.1	180	16	65.2	27.2	680	60		Wu et al. (2008)
Min River	14.9	37,000	3.0	3.3	260	9	45.9	19.1	480	18		Wu et al. (2008)
Huang River	23.2	146,000	9.0	1.1	90	13	22.0	9.2	230	34		Wu et al. (2008)
Wujiang	32.7	66,849	6.0	2.4	98	6	65	27.1	682	46		Han and Liu (2004)
Xijiang	363	437,000	9.2	3.4	54.9	24	69.1	28.8	647.6	283	4.6	Gaillardet et al. (1999)

A comparison of our results with earlier studies and other large rivers of the world is also shown. Drainage area was calculated by ArcGIS v. 10.0

Chemical weathering and CO_2 consumption rate

The contributions of silicate weathering, carbonate weathering, and evaporite dissolution to TDS in river water was calculated using the following equations (Xu and Liu 2007):

$$TDS_{sil} = [Na]_{sil} + [K]_{sil} + [Ca]_{sil} + [Mg]_{sil} + [SiO_2]_{sil} \quad (12)$$

$$TDS_{carb} = [Ca]_{carb} + [Mg]_{carb} + 1/2\,[HCO_3]_{carb} \quad (13)$$

$$TDS_{evap} = [Na]_{evap} + [Ca]_{evap} + [SO_4]_{evap} + [Cl]_{evap} \quad (14)$$

Together with information of drainage area and multi-year average discharge data from hydrologic yearbooks for each basin, chemical weathering rates of silicates, carbonates, and evaporite in the basins were estimated from the budget of silicate, carbonate, and evaporite weathering (Roy et al. 1999).

Silicate weathering rate (SWR) is calculated as

$$SWR = ([Na]_{sil} + [K]_{sil} + [Ca]_{sil} + [Mg]_{sil} + [SiO_2]_{sil}) \times \text{discharge/drainage area} \quad (15)$$

Carbonate weathering rate (CWR) is calculated as

$$CWR = ([Ca]_{carb} + [Mg]_{carb} + 1/2[HCO_3]_{carb}) \times \text{discharge/drainage area} \quad (16)$$

Evaporite dissolution rate (EWR) is calculated as

$$EWR = ([Na]_{evap} + [Ca]_{evap} + [SO_4]_{evap} + [Cl]_{evap}) \times \text{discharge/drainage area} \quad (17)$$

The influence of rock weathering on the consumption of atmospheric CO_2 must be considered with respect to time. In less than 10^5 years (the time required by rivers to transport dissolved C to the oceans), weathering of all lithologies is important for the consumption of CO_2 from the atmosphere. For a million years or more, C supplied by carbonate weathering is removed from the sea by calcite precipitation and soon returned to the atmosphere; therefore, CO_2 consumption from carbonate weathering can be neglected (Berner et al. 1983). We calculated CO_2 consumption rates ($\Phi[CO_2]$: mol km^{-2} a^{-1}) from silicate and carbonate weathering as follows (Roy et al. 1999).

The correlative equations via the data of cations, discharge, and drainage area of the rivers are

$$\Phi[CO_2]_{sil} = ([Na]_{sil} + [K]_{sil} + 2 \times [Ca]_{sil} + 2 \times [Mg]_{sil}) \times \text{discharge/drainage area} \quad (18)$$

$$\Phi[CO_2]_{carb} = ([Ca]_{carb} + [Mg]_{carb}) \times \text{discharge/drainage area} \quad (19)$$

The average of the last two mainstream samples in each basin was used to calculate rock weathering and CO_2 consumption rates, and the results are not significantly different from those calculated using average values of all the waters in each river. Average densities of 2.7 and 2.4 g cm^{-3} for silicate and carbonate were used to calculate erosion rate (Galy and France-Lanord 1999). Results of the calculation for rock weathering and CO_2 consumption rates for each basin are listed in Table 2.

In Jinshajiang evaporite (halite plus gypsum) dissolution was dominant with EWR of 29.5 t km^{-2} a^{-1}. Carbonate weathering is more important, with CWR of 42.7 and 22.5 t km^{-2} a^{-1} in Nujiang and Lancangjiang, respectively. The contributions of silicate weathering to total dissolved materials were minor compared with evaporite dissolution and carbonate weathering, with SWR of 1.8, 2.2, and 5.1 t km^{-2} a^{-1} in Jinshajiang, Lancangjiang, and Nujiang, respectively. The silicate weathering fluxes ranged from 0.25×10^6 to 0.44×10^6 t a^{-1}. We found that a total 1.14×10^6 t a^{-1} of dissolved materials originated from silicate weathering for the three rivers. This only represents <1 % of the global river drainage silicate weathering flux, 550×10^6 t a^{-1} (Gaillardet et al. 1999). However, total chemical denudation fluxes (including silicate, carbonate, and evaporite weathering) of the three rivers were 44.5–70.4 t km^{-2} a^{-1} (average 54.3 t km^{-2} a^{-1}), greater than published global mean weathering values of 24, 26, and 21 t km^{-2} a^{-1} (Meybeck 1979; Berner and Berner 1996; Gaillardet et al. 1999), respectively. This may indicate more intense chemical denudation of the three rivers draining the HQTP relative to those in the other areas of the world.

Calculated results of $\Phi[CO_2]_{sil}$ are 45.6×10^3, 84.9×10^3, and 157.5×10^3 mol km^{-2} a^{-1} for Jinshajiang, Lancangjiang, and Nujiang, respectively. The corresponding CO_2 consumption rates by carbonate weathering ($\Phi[CO_2]_{carb}$) are 157.8×10^3, 191.3×10^3, and 450.5×10^3 mol km^{-2} a^{-1}. Uncertainties in calculating the $(\sum \text{cation})_{sil}$ carry over to the flux calculations. Considering uncertainties of ±50 % in $(Ca/Na)_{sil}$ and $(Mg/K)_{sil}$ estimation, $\Phi[CO_2]_{sil}$ and $\Phi[CO_2]_{carb}$ are 25.5–37.3 $\times 10^9$ mol a^{-1} (213.4–313.1 $\times 10^3$ mol km^{-2} a^{-1}) and 92.3–99.8 $\times 10^9$ mol a^{-1} (770.9–821.1 $\times 10^3$ mol km^{-2} a^{-1}). Variability was about ±20 and ±4 % for $\Phi[CO_2]_{sil}$ and $\Phi[CO_2]_{carb}$, respectively, for the three rivers.

We assumed that all SO_4^{2-} was from evaporite (mainly gypsum) dissolution, which may overestimate $(\sum \text{cation})_{sil}$ and $\Phi[CO_2]_{sil}$, and underestimate $(\sum \text{cation})_{carb}$ and $\Phi[CO_2]_{carb}$. This is because sulfide oxidation can generate sulfuric acid (H_2SO_4), which can dissolve carbonate and silicate minerals without uptake of atmospheric CO_2. The assumption that all SO_4^{2-} was from evaporite (mainly gypsum) dissolution was based on reports of gypsum mines

Table 3 $\Phi[CO_2]_{sil}$ comparison of the TRR with other large rivers in orogenic zones

River name	TDS (mg/L)	CO_2 flux (10^9 mol a^{-1})	$\Phi[CO_2]_{sil}$ (10^3 mol km^{-2} a^{-1})	References
HQTP orogenic rivers				
Three rivers	76.1–479	33.5	34.2–179.9 (96)	This study
Three rivers	31–435	55	22–298 (109)	Noh et al. (2009)
Indus	17–641		~499	Pande et al. (1994)
Ganges	28–379	27	107–528 (250)	Galy and France-Lanord (1999)
Brahmaputra	90–110	105	115–253 (181)	Dalai et al. (2002), France-Lanord et al. (2003), Singh et al. (2005)
Upper Huang River	83–868	20	0.6–116 (88)	Wu et al. (2005)
Yarlung Tsangpo	16–356	21.7	17–35 (20)	Hren et al. (2007)
Non-HQTP orogenic rivers				
Amazon	~108	15–294 (102)	20–347 (262)	Edmond et al. (1996), Mortatti and Probst (2003)
Orinoco		4–28 (13)	74–255 (171)	Edmond et al. (1996)
Mackenzie	75–370	0.001–1.4 (0.2)	0.4–67 (13)	Edmond et al. (1996), Millot et al. (2003)
Yukon	190–240	0.8–1.5(1.1)	19–23 (21)	Millot et al. (2003)
Siberian	50–2101	0.09–0.6 (0.3)	18–20 (19)	Huh et al. (1998)
World average	25–2463	~8700	~900	Gaillardet et al. (1999), Krishnaswami et al. (1999)

Numbers in parentheses are average values

and gypsiferous red beds and our field observation in the basins (Wu et al. 2008). This information indicates that gypsum dissolution could be a major source of SO_4 in rivers. It is very difficult to distinguish gypsum dissolution and sulfide oxidation sources of SO_4 from the lithological makeup and major ion data. With exact mineralogical investigation of sulfate in the TRR, $\delta^{34}S$ values of dissolved sulfate could be used to trace whether sulfate comes from sulfide minerals or gypsum because those two usually have very different $\delta^{34}S$ values (Hoefs 1997).

Given these uncertainties, however, total CO_2 consumption fluxes from silicate and carbonate weathering were, respectively, 33.5×10^9 and 96.6×10^9 mol a^{-1} in the three rivers, accounting for about 0.4 and 0.8 % of corresponding global total CO_2 consumption fluxes (8700×10^9 and $12{,}300 \times 10^9$ mol a^{-1}) (Gaillardet et al. 1999). The three basins are responsible for ~0.5 % of global water discharge to oceans, and 0.4 % of global continental area (Gaillardet et al. 1999). Thus, the contribution of the three rivers to global CO_2 consumption is commensurate with their drainage area and water discharge. This also demonstrates that chemical weathering of the three rivers draining the HQTP makes only a minor contribution to the reduction of atmospheric CO_2 content.

Worldwide comparison

We compared SWR, CWR, EWR, $\Phi[CO_2]_{sil}$, and $\Phi[CO_2]_{carb}$ from the present study of the TRR to earlier ones and from other large rivers in the world (Tables 2, 3).

Table 2 shows that estimated rock weathering and CO_2 consumption rates in our study are generally smaller than those estimated for the seven rivers by Wu et al. (2008). In particular, our estimates of SWR, $\Phi[CO_2]_{sil}$, CWR, and $\Phi[CO_2]_{carb}$ for Jinshajiang are clearly smaller than those of Wu et al. (2008). Reasons could be as follows. First, the drainage area used for estimating rock weathering and CO_2 consumption rates vary between the two studies. Second, by comparing ion data from Jinshajiang basin between the studies, the Na concentration of 2391 μmol L^{-1} in Wu et al. (2008) is higher than our value (an average 1789 μmol L^{-1} for the last two mainstream samples), and the Cl concentration of 1269 μmol L^{-1} in Wu et al. (2008) is lower than our figure (an average 1690 μmol L^{-1} for the last two mainstream samples). Assuming that Na_{sil} equals Na_{river} minus Cl_{evap} and Na_{rain}, Ca_{sil} estimation using an appropriate $(Ca/Na)_{sil}$ gave greater Na_{sil} and Ca_{sil} in Wu et al. (2008) than our study. Therefore, the estimated SWR, CWR, $\Phi[CO_2]_{sil}$, and $\Phi[CO_2]_{carb}$ of Wu et al. (2008) are

greater than our values. The different measured Na and Cl concentrations between the two works may be related to uneven distributions of halite minerals across the three river basins. The rapid dissolution of halite after random rainfall may greatly increase Na and Cl concentrations in river waters near the halite materials. To overcome this, long-term field observation of water chemistry and more samples for calculating average values of rock weathering and CO_2 consumption rates may be needed. The final reason for the discrepancy may be that unlike our study, Wu et al. (2008) calculated the total weathering rates of carbonate and evaporite for Jinshajiang, Lancangjiang, and Nujiang.

In comparison with other large rivers, similar SWR values were found in the Nujiang, Wujiang, Lancangjiang, and Min River (Han and Liu 2004; Wu et al. 2008). The Jinshajiang and Xijiang had similar values of $\Phi[CO_2]_{sil}$ in terms of flux (10^3 mol km^{-2} a^{-1}) (Gaillardet et al. 1999). The Langcangjiang and Huang River had similar CWR, $\Phi[CO_2]_{sil}$, and $\Phi[CO_2]_{carb}$ in terms of flux (10^3 mol km^{-2} a^{-1}) (Wu et al. 2008). Nujiang had a CWR similar to the Min and Yalong Rivers (Wu et al. 2008). The Min, Huang, and Yalong Rivers are all on the eastern HQTP, with landscapes, vegetation coverage, and populations similar to the TRR. The Wujiang and Xijiang Rivers are in southwestern China and drain a typical carbonate rock area, and carbonate weathering was a major contributor to dissolved materials in river water.

Gaillardet et al. (1999) quoted data of Jinshajiang (Changjiang) and Lancangjiang (Mekong) from near the river mouths. They calculate larger values of SWR, CWR, $\Phi[CO_2]_{sil}$, and $\Phi[CO_2]_{carb}$ than our estimates.

However, their estimates may be not suitable for evaluation of the impact of chemical weathering of the HQTP on global climate, because the lower courses of their studied rivers flow through heavily populated plains and hence may be polluted by industrialized and agricultural activities. Meanwhile, many tributaries not originating on the HQTP and some irrigation ditches flow into the main channels in the lower courses of these rivers. Therefore, the estimated chemical weathering may be inadequate due to considerable anthropogenic impacts on chemical compositions of river water in those areas.

The net CO_2 consumption by silicate weathering ($\Phi[CO_2]_{sil}$) was from 45.6 $\times$ 10^3 to 157.5 $\times$ 10^3 mol km^{-2} a^{-1}, with an average of 96 $\times$ 10^3 mol km^{-2} a^{-1} in the TRR. Our average $\Phi[CO_2]_{sil}$ is near the estimated 88 $\times$ 10^3 mol km^{-2} a^{-1} for the upper Huang River by Wu et al. (2005), slightly smaller than the average 109 $\times$ 10^3 mol km^{-2} a^{-1} for the TRR estimated by Noh et al. (2009), but much smaller than values for the Indus, Ganges and Brahmaputra draining the HQTP south flank and the Amazon and Orinoco draining the Andes Mountains. In the Ganges and Brahmaputra, the contribution of silicate weathering is large (20–30 % of cations in river water) and water discharge of the two rivers is substantial, therefore net CO_2 consumption rates are accordingly higher (Dalai et al. 2002). The high chemical weathering rates were attributed to strong physical erosion caused by strong precipitation and extreme topography (Singh et al. 2005). The Mackenzie draining the western Canadian orogenic belt (Rocky and Mackenzie Mountains) has relatively small CO_2 consumption fluxes, likely owing to the low exposure of silicates and low temperatures (Millot et al. 2003).

Conclusions

The Jinshajiang, Lancangjiang, and Nujiang had variable major ion compositions, with TDS = 76.1–479 mg/L, reflecting the complex geologic makeup of the three drainage basins. Ca and HCO_3 were the most abundant cation and anion, respectively, in the water samples, primarily reflecting the weathering of carbonates. Cl, SO_4, and Na dominated the major element compositions in the mainstream samples of the Jinshajiang, indicating that evaporite dissolution was the major contributor to ionic compositions. On average, silicate weathering contributed $\sim$13 % to total cations. Some samples of the Nujiang near the Tengchong Volcano showed distinctive silicate weathering signatures.

Calculation of chemical weathering rates based on a forward model showed that carbonate weathering was dominant, with rates of 22.5 and 42.7 t km^{-2} a^{-1} in Lancangjiang and Nujiang, respectively. In Jinshajiang, evaporite dissolution was important and had a rate of 29.5 t km^{-2} a^{-1}. The contributions of silicate weathering to total dissolved materials were minor, with rates of 1.8, 2.2, and 5.1 t km^{-2} a^{-1} in Jinshajiang, Lancangjiang, and Nujiang, respectively. The more intense silicate weathering in the Nujiang basin may be related to abundant volcanic rocks and granites in that basin. Long-term average CO_2 consumption by silicate weathering was 96 $\times$ 10^3 mol km^{-2} a^{-1}, much smaller than values of the Indus, Ganges, and Brahmaputra draining the south flank of HQTP and the Amazon and Orinoco draining the Andes Mountains. Silicate and carbonate weathering in the Jinshajiang, Lancangjiang, and Nujiang basins on the HQTP consumed 33.5 $\times$ 10^9 and 96.6 $\times$ 10^9 mol a^{-1} of atmospheric CO_2, respectively, making up 0.4 and 0.8 % of global total CO_2 consumption fluxes by silicate and carbonate weathering. This demonstrates that chemical weathering of the three rivers draining the HQTP has only a minor contribution to reducing the CO_2 content of the atmosphere. However, the average total chemical weathering flux (including silicate, carbonate, and evaporite weathering) of the three rivers is 54.3 t km^{-2} a^{-1}, greater

than the published global mean value of ~ 24 t km^{-2} a^{-1}. This suggests a more intense chemical weathering for the three rivers draining the HQTP than in the other areas of the world.

Acknowledgments The authors thank two anonymous reviewers for helpful comments and suggestions that greatly improved the manuscript. This work was supported jointly by the Ministry of Science and Technology of China through the National Basic Research Program of China ('973' Program, Grant No. 2013CB956401), and by the National Natural Science Foundation of China (Grant Nos. 41210004, 41130536, 41173030, 41463004, 41372376).

References

Berner EK, Berner RA (1996) Global environment: water, air and geochemical cycles. Prentice-Hall, USA

Berner RA, Lassaga AC, Garrels RM (1983) The carbonate–silicate geochemical cycle and its effect on atmospheric carbon dioxide over the past 100 million years. Am J Sci 284:1183–1192

Bickle MJ, Bunbury J, Chapman HJ et al (2003) Fluxes of Sr into the headwaters of the Ganges. Geochim Cosmochim Acta 67:2567–2584

Bickle MJ, Chapman HJ, Bunbury J et al (2005) Relative contributions of silicate and carbonate rocks to riverine Sr fluxes in the headwaters of the Ganges. Geochim Cosmochim Acta 69:2221–2240

Blum JD, Gazis CA, Jacobson AD et al (1998) Carbonate versus silicate weathering in the Raikhot watershed within the High Himalayan Crystalline Series. Geology 26:411–414

Burbank DW, Blythe AE, Putkonen J et al (2003) Decoupling of erosion and precipitation in the Himalayas. Nature 426:652–655

Bureau of Geology and Mineral Resources of Qinghai Province (1990) Regional Geology of Qinghai Province. Geological Publishing House, Beijing **(in Chinese)**

China Geological Survey (2004) The 1:2,500,000 Geological Map of China. China Cartographic Publishing House, Beijing **(in Chinese)**

Dalai TK, Krishnaswami S, Sarin MM (2002) Major ion chemistry in the headwater of the Yamuna river system: chemical weathering, its temperature dependence and CO_2 consumption in the Himalaya. Geochimca Cosmochim Acta 66:3397–3416

Edmond JM (1992) Himalayan tectonics, weathering processes, and the strontium isotope record in marine limestones. Science 258:1594–1597

Edmond JM, Palmer MR, Measures CI et al (1995) The fluvial geochemistry and denudation rate of the Guayana Shield in Venezuela, Colombia and Brazil. Geochimca Cosmochim Acta 59:3301–3325

Edmond JM, Palmer MR, Measures CI et al (1996) Fluvial geochemistry of the eastern slope of the northeastern Andes and its foredeep in the drainage of the Orinoco in Colombia and Venezuela. Geochimca Cosmochim Acta 60:2949–2974

France-Lanord C, Evans M, Hurtrez JE et al (2003) Annual dissolved fluxes from Central Nepal rivers: budget of chemical erosion in the Himalayas. CR Geosci 335:1131–1140

Frenzel B, Li J, Liu SJ (1995) On the upper quaternary paleoecology of Eastern Tibet-Preliminary results of an expedition to the Eastern Tibetan Plateau, 1992. Sci China (Ser B) 38(4):484–494

Fu DQ, Wang XH, Liu J et al (1998) The investigation and analysis about background value of water environmental in the source area of Yangtze River. Environ Monit China 14(1):9–11 **(In Chinese with English abstract)**

Gaillardet J, Duprè B, Louvat P et al (1999) Global silicate weathering and CO_2 consumption rates deduced from the chemistry of large rivers. Chem Geol 159:3–30

Galy A, France-Lanord C (1999) Weathering processes in the Ganges-Brahmaputra basin and the riverine alkalinity budget. Chem Geol 159:31–60

Galy A, France-Lanord C (2001) Higher erosion rates in the Himalayas: geochemical constraints on riverine fluxes. Geology 29:23–26

Hallet B, Molnar P (2001) Distorted drainage basins as markers of crustal strain east of the Himalaya. J Geophys Res 206:13697–13709

Han GL, Liu CQ (2004) Water geochemistry controlled by carbonate dissolution: a study of the river waters draining karst-dominated terrain, Guizhou province, China. Chem Geol 204:1–21

Hoefs J (1997) Stable isotope geochemistry. Springer, Berlin

Holt WE, Ni JF, Wallace TC et al (1991) The active tectonics of the Eastern Himalayan Syntaxis and surrounding regions. J Geophys Res 96:14595–14632

Hren MT, Chamberlain CP, Hilley GE et al (2007) Major ion chemistry of the Yarlung-Brahmaputra river: chemical weathering, erosion, and CO_2 consumption in the southern Qinghai-Tibet Plateau and eastern syntaxis of the Himalaya. Geochim Cosmochim Acta 71:2907–2935

Huang X, Sillanpää M, Gjessing ET et al (2009) Water quality in the Tibetan Plateau: major ions and trace elements in the headwaters of four major Asian rivers. Sci Total Environ 407:6242–6254

Huh Y, Panteleyev G, Babich D et al (1998) The fluvial geochemistry of the rivers of Eastern Siberia: Π. Tributaries of the Lena, Omoloy, Yana, Indigirka, Kolyma, and Anadyr draining the collisional/accretionary zone of the Verkhoyansk and Cherskiy ranges. Geochim Cosmochim Acta 62:2053–2075

Jiang L, Yao Z, Wang R et al (2015) Hydrochemistry of the middle and upper reaches of the Yarlung Tsangpo River system: weathering processes and CO_2 consumption. Environ Earth Sci. doi:10.1007/s12665-015-4237-6

Karim A, Veizer J (2000) Weathering processes in the Indus River Basin: implications from riverine varbon, sulfur, oxygen, and strontium isotopes. Chem Geol 170:153–177

Krishnaswami S, Singh SK, Dalai TK (1999) Silicate weathering in the Himalaya: role in contributing to major ions and radiogenic Sr to the Bay of Bengal. In: Somayajulu BLK (ed) Ocean science, trends and future directions. Indian National Science Academy and Academia International, New Delhi, pp 23–51

Li XD, Liu CQ, Liu XL et al (2011) Identification of dissolved sulfate sources and the role of sulfuric acid in carbonate weathering using dual-isotopic data from the Jialing River, Southwest China. J Asian Earth Sci 42:370–380

Li SL, Chetelat B, Yue F et al (2014) Chemical weathering processes in the Yalong River draining the eastern Tibetan Plateau, China. J Asian Earth Sci 88:74–84

Liu B, Liu CQ, Zhang G et al (2013) Chemical weathering under mid- to cool temperature and monsoon-controlled climate: a study on water geochemistry of the Songhuajiang River system, northeast China. Appl Geochem 31:265–278

Meybeck M (1979) Concentrations des eaux fluviales en éléments majeurs et apports en solution aux océans. Revue de Geologie Dynamique et de Geographie Physique 21:215–246

Meybeck M (1987) Global chemical weathering of surficial rocks estimated from river dissolved loads. Am J Sci 287:401–428

Meybeck M (2003) Global occurrence of major elements in rivers. In: Drever JI (ed) Treatise on geochemistry. Elsevier, Netherland, pp 207–223

Millot R, Gaillardet J, Dupré B et al (2003) Northern latitude chemical weathering rates: clues from the Mackenzie River Basin. Geochim Cosmochim Acta 67:1305–1329

Moon S, Huh Y, Qin JH et al (2007) Chemical weathering in the Hong (Red) River basin: rates of silicate weathering and their controlling factors. Geochim Cosmochim Acta 71:1411–1430

Mortatti J, Probst JL (2003) Silicate rock weathering and atmospheric/soil CO_2 uptake in the Amazon basin estimated from river water geochemistry. Chem Geol 197:177–196

Negrel P, Allègre CJ, Dupré B et al (1993) Erosion sources determined by inversion of major and trace element ratios and strontium isotopic ratios in river water: the Congo Basin case. Earth Planet Sci Lett 120:59–76

Noh H, Huh Y, Qin JH et al (2009) Chemical weathering in the Three Rivers region of Eastern Tibet. Geochim Cosmochim Acta 73:1857–1877

Oliver L, Harris N, Bickle M et al (2003) Silicate weathering rates decoupled from the 87Sr/86Sr ratio of the dissolved load during Himalayan erosion. Chem Geol 201:119–139

Pande K, Sarin MM, Trivedi JR et al (1994) The Indus system (India-Pakistan): major ion chemistry, uranium and strontium isotopes. Chem Geol 116:245–259

Qin JH, Huh Y, Edmond JM et al (2006) Chemical and physical weathering in the Min Jiang, a headwater tributary of the Yangtze River. Chem Geol 227:53–69

Rai SK, Singh SK, Krishnaswami S (2010) Chemical weathering in the plain and peninsular sub-basins of the Ganga: impact on major ion chemistry and elemental fluxes. Geochim Cosmochim Acta 74:2340–2355

Raymo ME, Ruddiman WF (1992) Tectonic forcing of late Cenozoic climate. Nature 359:117–122

Roy S, Gaillardet J, Allègre CJ (1999) Geochemistry of dissolved and suspended loads of the Seine river, France: anthropogenic impact, carbonate and silicate weathering. Geochim Cosmochim Acta 63:1277–1292

Shui XJ, Yang Y, Yang F et al (2006a) Challenge to the source of Chang Jiang: Tuotuo River. Huaxia Geogr 11:22–51 **(in Chinese with English abstract)**

Shui XJ, Yang Y, Yang F et al (2006b) Chumaer River: intrude blank area of scientific research. Huaxia Geogr 12:98–121 **(in Chinese with English abstract)**

Singh SK, Sarin MM, France-Lanord C (2005) Chemical erosion in the eastern Himalaya: major ion composition of the Brahmaputra and ^{13}C of dissolved inorganic carbon. Geochim Cosmochim Acta 69:3573–3588

Tapponnier P, Peltzer G, Le Dain AY et al (1982) Propagating extrusion tectonics in Asia: new insights from simple experiments with plasticine. Geology 10:611–616

Tian H, Wang S, Liu J et al (2006) Patterns of soil nitrogen storage in China. Global Biogeochem Cycles. doi:10.1029/2005GB002464

Wang E, Burchfiel BC (2000) Late Cenozoic to Holocene deformation in southwestern Sichuan and adjacent Yunnan, China, and its role in formation of the southeastern part of the Tibetan Plateau. Geol Soc Am Bull 112:413–423

Wang X, Metcalfa I, Jian P et al (2000) The Jinshajiang-Ailaoshan suture zone, China: tectonostratigraphy, age and evolution. J Asian Earth Sci 18:675–690

Wang ZL, Zhang J, Liu CQ (2007) Strontium isotopic compositions of dissolved and suspended loads from the main channel of the Yangtze River. Chemosphere 69:1081–1088

Weyerhaeuser H, Wilkes A, Kahrl F (2005) Local impacts and responses to regional forest conservation and rehabilitation programs in China's northwest Yunnan province. Agric Syst 85:234–253

Wu H, Boulter CA, Ke B et al (1995) The Changning-Menglian suture zone; a segment of the major Cathaysian-Gondwana divide in Southeast Asia. Tectonophysics 242:267–280

Wu LL, Huh Y, Qin JH et al (2005) Chemical weathering in the Upper Huang He (Yellow River) draining the eastern Qinghai Plateau. Geochim Cosmochim Acta 69:5279–5294

Wu W, Xu S, Yang J et al (2008) Silicate weathering and CO2 consumption deduced from the seven Chinese rivers originating in the Qinghai-Tibet Plateau. Chem Geol 249:307–320

Xu ZF, Liu CQ (2007) Chemical weathering in the upper reaches of Xijiang River draining the Yunnan-Guizhou Plateau, Southwest China. Chem Geol 239:83–95

Yu SS, Tang Y (1981) The hydrochemical characteristics of the saline lakes on the Qinghai-Xizang Plateau. Oceanologia et Limnologia Sinica 12(6):498–511 **(in Chinese with English abstract)**

Zhang DD, Peart M, Jim CY et al (2003) Precipitation chemistry of Lhasa and other remote towns, Tibet. Atmos Environ 37:231–240

Zhao JC, Geng DQ, Peng JH et al (2003) Origin of major elements and Sr isotope for river water in Yangtze River source area. Hydrogeol Eng Geol 2:89–98 **(in Chinese with English abstract)**